Springer

Acta Mechanica Sinica

CrossMark click for updates

• RESEARCH PAPER •

Acta Mech. Sin., Vol. 40, 223274 (2024)
https://doi.org/10.1007/s10409-023-23274-x

Rotating MHD flow and heat transfer of generalized Maxwell fluid through an infinite plate with Hall effect

Yanli Qiao, Huanying Xu, and Haitao Qi*

School of Mathematics and Statistics, Shandong University, Weihai 264209, China

Received November 20, 2023; accepted December 13, 2023; published online May 16, 2024

Research on the flow and heat transfer characteristics of viscoelastic fluids has been an issue of considerable interest. However, it is gradually found that the behaviors of some viscoelastic fluids deviate from the classical flow and heat transfer phenomena, which are represented by integer order governing equations. Thus, it is necessary to construct a new constitutive relationship to study complex viscoelastic fluids. In this paper, we investigate the rotating magnetohydrodynamics (MHD) flow and heat transfer of generalized Maxwell fluid with distributed order characteristics over an infinite plate, and the Hall effect is considered. In view of the multi-scale characteristics and nonlocality of generalized Maxwell fluid flow and heat transfer, fractional calculus is introduced to accurately depict the flow and heat transfer mechanism. Fractional governing equations consisting of the distributed order time fractional momentum equations and time fractional energy equation are derived. To calculate the numerical solutions of velocities and temperature governing equations, the Crank-Nicolson finite difference schemes are proposed based on the L1 approximation formula. Then, the effectiveness and feasibility of the numerical method are verified, and the effects of relevant parameters on fluid velocities and temperature are discussed, graphically. Finally, some conclusions are summarized.

Generalized Maxwell fluid, Magnetohydrodynamics flow, Hall effect, Fractional calculus, Finite difference method

Citation: Y. Qiao, H. Xu, and H. Qi, Rotating MHD flow and heat transfer of generalized Maxwell fluid through an infinite plate with Hall effect, Acta Mech. Sin. **40**, 223274 (2024), https:// doi.org/10.1007/s10409-023-23274-x

1. Introduction

Viscoelastic fluids play an important role in the development of social production. Research on the essential properties of viscoelastic fluids makes the application of fluids more extensive. Therefore, to further promote the practical application of viscoelastic fluids, flow and heat transfer processes of the fluid under the action of electric field, magnetic field and pressure gradient are concerned and studied [1-5]. Moreover, due to the extensive existence of magnetic field in modern technology and human life, such as magnetohydrodynamic generators, magnetohydrodynamic accelerators, even some tissues and organs in the human body, it is found that the effects of magnetic field on the flow of viscoelastic fluids are worth studying. Thus, magnetohydrodynamic has developed rapidly [6-9]. And the influence of Hall current on magnetohydrodynamics (MHD) flow is also received attention and relevant research has been carried out. Hayat et al. [10] constructed the Oldroyd-B fluid model to describe the behavior of non-Newtonian fluids and discussed the effect of Hall current on the rotational flow of non-Newtonian fluid in porous media. Veerakrishna et al. [11] discussed the effects of radiation and Hall current on the unsteady MHD free convective flow in a vertical channel filled with a porous medium. Rasheed et al. [12] investigated the two-dimensional MHD free convection of Casson fluid on the vertical surface with transverse magnetic field, viscous dissipation, and Hall current.

Recently, fractional calculus theory is introduced to describe the flow and heat transfer of viscoelastic fluids showing non-Newtonian fluid characteristics, which is unable to be described by integral calculus theory. And it is proven

*Corresponding author. E-mail address: htqi@sdu.edu.cn (Haitao Qi)
Executive Editor: Mingjiu Ni

that the fractional differential operators with nonlocality and memory can be used to characterize some complex motion processes of the fluids. Yin and Zhu [13] analyzed the unidirectional oscillating flow of the fractional Maxwell fluid through an infinite straight pipe driven by a periodic pressure gradient. Zhao et al. [14] developed the fractional boundary layer governing equations with mixed space-time derivatives. Chen et al. [15] investigated the boundary layer flow of viscoelastic magnetic fluid on a stretched thin plate by using a double fractional Maxwell model. Moosavi et al. [16] applied the Maxwell fractional order model to study the unsteady flow and natural convection heat transfer of viscoelastic non-Newtonian fluid on vertical forward step. They verified that the fractional derivative can be used to describe the fluid properties more accurately. And then, complex viscoelastic fluids has been developed rapidly based on the fractional derivative and more information can be referred to Refs. [17-20].

Furthermore, more complex systems are concerned with the advancement of research. A new fractional calculus operator, known as the distributed order fractional derivative, is introduced to describe the physical phenomena, such as mechanical behavior of viscoelastic materials with spatially varying properties [21], memory effects in composite materials [22], multi-scale effects [23]. For the flow and heat transfer behaviors of viscoelastic fluids with multi-scale characteristics, the distributed order fractional derivative is applied to accurately describe the complex interaction and superposition process of nonlocal effects and memory effects. Atanackovic [24] presented the constitutive model of viscoelastic body with distributed order fractional derivative dissipation under the linear stress state. We observed that the construction of the model took into account all derivatives of stress and strain between zero and one with the weight function. Duan and Qiu [25] studied the steady periodic flow of Stokes' second problem for viscoelastic fluid based on the constitutive equation with distributed order derivative. Yang et al. [26] firstly established a distributed space fractional constitutive equation to study the flow and heat transfer of viscoelastic fluid in the boundary layer. Then, Yang et al. [27] proposed a new distributed time fractional constitutive model for the unsteady natural convection boundary layer flow and heat transfer under the influence of magnetic field. And taken into account the viscous dissipation and Joule heating, the effect of alternating field on the electroosmotic flow and heat transfer of generalized Maxwell fluid with distributed order time fractional characteristics was investigated in Refs. [28, 29].

In addition, it is worth noting that the flow and heat transfer models of viscoelastic fluids with fractional derivative and distributed order fractional derivative often consist of multiple fractional operators. So it is difficult to quantitatively study the behaviors of complex viscoelastic fluids. This is because the analytical solutions of the fractional models are hard to be given directly. Thus, the emergence of numerical solutions provides a new idea for the study of fractional models [30, 31] and the construction of numerical methods has become a hot issue. For instance, Wu [32] studied the Stokes' first problem of a heated generalized second-order fluid with fractional derivative by using the implicit numerical approximation scheme and proved the stability and convergence of the numerical scheme. Yang et al. [33] presented the electroosmotic flow of fractional Maxwell fluid through the rectangular microchannel and proposed a fully discrete spectral method based on time difference method and spatial Legendre spectral method. Zhao [34] presented a new fractional finite volume method for the mixed convection boundary layer flow and heat transfer of viscoelastic fluid on a flat plate by combining the shifted Grünwald-Letnikov formula. Meng et al. [35] showed the finite difference scheme of the flow, heat and mass transfer equations of viscoelastic fluid in porous media based on the fractional constitutive model. And we also carried out some numerical analysis for the flow and heat transfer of viscoelastic fluids. The finite difference algorithms were also developed to calculate the numerical solutions of the nonlinear coupled governing equations of velocity and temperature for the generalized Maxwell fluids [36, 37].

However, we find that the relevant research for complex viscoelastic fluids is still relatively rare and Hall effect, defined as the ratio between the electron-cyclotron frequency and the electron-atom collision frequency, can not be ignored when the fluid density is low or the applied magnetic field is strong [10]. Thus, we investigate the MHD flow and heat transfer of generalized Maxwell fluid with distributed order characteristics in the rotating framework, in which a strong magnetic field is considered. The paper is organized as follows. In Sect. 2, some preliminaries are given and the corresponding distributed order time fractional governing equations of the fluid flow and heat transfer are constructed. The numerical method for solving the governing equations is established in Sect. 3. The validity of the numerical method is verified and the effects of related model parameters on the fluid velocities and temperature are discussed in Sect. 4. Finally, some conclusions are given in Sect. 5.

2. Mathematical formulation

The rotating MHD flow and heat transfer of the generalized Maxwell fluid with Hall effect through an infinite straight plate are considered. As shown in Fig. 1, a Cartesian

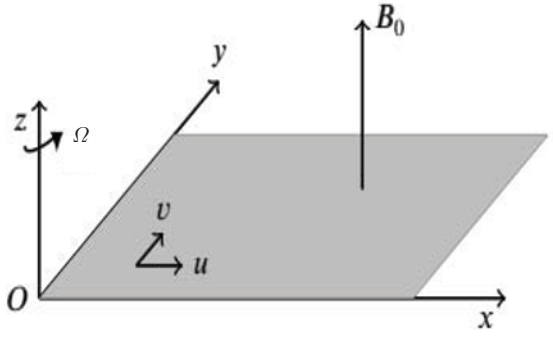

Figure 1 Physical sketch of the model.

coordinate system (x, y, z) is established by taking a vertex of the plate as the origin O. xOy plane is parallel to the plate and z-axis is perpendicular to the plate. The strong magnetic field with intensity B_0 is applied along the z-axis direction. Here, we assume that the fluid and the plate are at rest at the temperature T_∞ initially, and then the whole system rotates around the z-axis at the angular velocity $\mathbf{\Omega}$= $(0, 0, \Omega)$.

Considering that the generalized Maxwell fluid rotates around the z-axis together with the infinite plate and the fluid has no vertical movement, we assume that the flow parameters depend only on z and t, thus the velocity field can be defined as $\mathbf{V}$= $(u(z,t), v(z,t), 0)$. For the incompressible viscoelastic fluid, the continuity equation,

$$\nabla \cdot \mathbf{V} = 0, \tag{1}$$

is satisfied, and the momentum equation is

$$\begin{aligned}&\rho\left[\frac{\mathrm{d}\mathbf{V}}{\mathrm{dt}} + 2\mathbf{\Omega}\times\mathbf{V} + \mathbf{\Omega}\times(\mathbf{\Omega}\times\mathbf{r})\right]\\ &= -\nabla p + \nabla\cdot\mathbf{S} + \mathbf{J}\times\mathbf{B} + \rho\mathbf{g}\beta_T(T - T_\infty),\end{aligned} \tag{2}$$

where $\rho, p, \beta_T, \mathbf{S}, \mathbf{J}$, and $\mathbf{g}$ are the fluid density, fluid pressure, coefficient of thermal expansion, shear stress tensor, current density and acceleration of the gravity, respectively. $\mathbf{B} = (0, 0, B_0)$ is the total magnetic field and $\mathbf{r}$= (x, y, z) is the radial coordinate. The generalized Ohm's law for a strong magnetic field is derived, shown as [38, 39]

$$\mathbf{J} + \frac{\omega_e\tau_e}{B_0}(\mathbf{J}\times\mathbf{B}) = \sigma\left(\mathbf{E} + \mathbf{V}\times\mathbf{B} + \frac{1}{en_e}\nabla p_e\right), \tag{3}$$

in which $\mathbf{E}$ is the electric field, ω_e is the cyclotron frequency of electron, τ_e is the electron collision time, σ is the electrical conductivity, e is the electron charge, $1/(en_e)$ is the Hall factor, n_e is the number density of the electrons, and p_e is the electron pressure.

Assuming the electric field $\mathbf{E} = 0$, and neglecting the electron pressure gradient, the ion-slip and thermo-electric effects in Eq. (3), we have

$$\mathbf{J}\times\mathbf{B} = \frac{\sigma B_0^2}{1+m^2}(mv - u)\mathbf{i} - \frac{\sigma B_0^2}{1+m^2}(v + mu)\mathbf{j}, \tag{4}$$

where $m = \omega_e\tau_e$ is the Hall parameter.

For the generalized Maxwell fluid with time distributed order characteristics, the modified constitutive relationship is presented to depict flow behavior of the fluid,

$$\mathbf{S} + \int_0^1 \varpi(\alpha)\lambda^\alpha\, {}_0D_t^\alpha\mathbf{S}\mathrm{d}\alpha = \mu\mathbf{A}, \tag{5}$$

in which $\mathbf{A} = \mathbf{L} + \mathbf{L}^\mathbf{T}$ is the first Rivlin-Ericksen tensor, $\mathbf{L}$ is the velocity gradient, λ is the relaxation time and μ is the viscosity coefficient of the fluid. ${}_0D_t^\alpha$ is the Caputo fractional derivative operator of order α, defined as

$${}_0D_t^\alpha f(z,t) = \frac{1}{\Gamma(1-\alpha)}\int_0^t (t-\tau)^{-\alpha}\frac{\partial f(z,\tau)}{\partial\tau}\mathrm{d}\tau, \tag{6}$$

and the distributed order time fractional derivatives is

$$\mathcal{D}_t^\varpi f(x,t) = \int_0^1 \varpi(\alpha)\, {}_0D_t^\alpha f(x,t)\mathrm{d}\alpha, \tag{7}$$

where $f(z,t)$ is a function of z and t, $\varpi(\alpha)$ is the weight function satisfing $\varpi(\alpha) \geq 0$ and $\int_0^1 \varpi(\alpha)\mathrm{d}\alpha = 1$. Then, the distributed order time fractional constitutive model of generalized Maxwell fluid can be rewritten as

$$\begin{aligned}S_{xz} + \int_0^1 \varpi(\alpha)\lambda^\alpha\, {}_0D_t^\alpha S_{xz}\mathrm{d}\alpha &= \mu\frac{\partial u}{\partial z},\\ S_{yz} + \int_0^1 \varpi(\alpha)\lambda^\alpha\, {}_0D_t^\alpha S_{yz}\mathrm{d}\alpha &= \mu\frac{\partial v}{\partial z},\end{aligned} \tag{8}$$

and $S_{xx} = S_{yy} = S_{xy} = S_{zz} = 0$.

Substituting Eqs. (4) and (8) into Eq. (2), we obtain the governing equations of the velocity distribution for viscoelastic fluid,

$$\begin{aligned}&\rho\left[\frac{\partial u}{\partial t} + \int_0^1 \varpi(\alpha)\lambda^\alpha\, {}_0D_t^{1+\alpha}u\mathrm{d}\alpha\right]\\ &- 2\rho\Omega\left[v + \int_0^1 \varpi(\alpha)\lambda^\alpha\, {}_0D_t^\alpha v\mathrm{d}\alpha\right]\\ &= \mu\frac{\partial^2 u}{\partial z^2} - \left[\frac{\partial p'}{\partial x} + \int_0^1 \varpi(\alpha)\lambda^\alpha\, {}_0D_t^\alpha\left(\frac{\partial p'}{\partial x}\right)\mathrm{d}\alpha\right]\\ &\quad + \frac{\sigma B_0^2}{1+m^2}\left[(mv-u) + \int_0^1 \varpi(\alpha)\lambda^\alpha\, {}_0D_t^\alpha(mv-u)\mathrm{d}\alpha\right]\\ &\quad + \rho g\beta_T\left[(T - T_\infty) + \int_0^1 \varpi(\alpha)\lambda^\alpha\, {}_0D_t^\alpha(T-T_\infty)\mathrm{d}\alpha\right],\end{aligned} \tag{9}$$

$$\begin{aligned}&\rho\left[\frac{\partial v}{\partial t} + \int_0^1 \varpi(\alpha)\lambda^\alpha\, {}_0D_t^{1+\alpha}u\mathrm{d}\alpha\right]\\ &+ 2\rho\Omega\left[u + \int_0^1 \varpi(\alpha)\lambda^\alpha\, {}_0D_t^\alpha u\mathrm{d}\alpha\right]\end{aligned} \tag{10}$$

$$= \mu\frac{\partial^2 v}{\partial z^2} - \left[\frac{\partial p'}{\partial y} + \int_0^1 \varpi(\alpha)\lambda^\alpha\, {}_0D_t^\alpha\left(\frac{\partial p'}{\partial y}\right)\mathrm{d}\alpha\right] - \frac{\sigma B_0^2}{1+m^2}\left[(v+mu) + \int_0^1 \varpi(\alpha)\lambda^\alpha\, {}_0D_t^\alpha(v+mu)\mathrm{d}\alpha\right],$$

where p' refers to the modified pressure defined as $p' = p - \rho\Omega^2(x^2+y^2)/2$. Distributed order fractional operators are used to characterize the flow process of complex fluids with time multi-scale effects. When the weight function $\varpi(\alpha)$ is Dirac delta function, Eqs. (9) and (10) will degenerate into a general time fractional order equations, which can describe the memory and heredity of the flow process.

The following initial and boundary conditions are considered:

$$\begin{aligned} t = 0 &: \begin{cases} u(z,0) = 0, & v(z,0) = 0, \\ \frac{\partial u(z,0)}{\partial t} = 0, & \frac{\partial v(z,0)}{\partial t} = 0, \end{cases} \\ t > 0 &: \begin{cases} u(0,t) = U_0 e^{-at}, & v(0,t) = 0, \quad z = 0, \\ u(z,t) \to 0, & v(z,t) \to 0, \quad z \to \infty, \end{cases} \end{aligned} \tag{11}$$

where U_0 is the characteristic velocity.

Furthermore, the temperature distribution of the generalized Maxwell fluid is investigated. Taken into account the flow characteristics and thermal memory of the fluid, the Caputo time fractional derivative is introduced to depict the heat transfer effect of the fluid. The time fractional SPL heat conduction equation are developed by using the fractional Taylor's series expansion based on the single-phase-lag model [40, 41],

$$\left(1 + \tau_q^\gamma\, {}_0D_t^\gamma\right)\mathbf{q}(z,t) = -\kappa\nabla T(z,t), \quad 0 < \gamma < 1, \tag{12}$$

where $\mathbf{q}$ is the heat flux, κ is the thermal conductivity, τ_q is the relaxation time of heat flux, and γ is the order of Caputo fractional derivative.

The energy equation with viscous dissipation, Joule heat and thermal radiation is presented,

$$\rho c\left(\frac{\partial T}{\partial t} + \mathbf{V}\cdot\nabla T\right) = -\nabla\cdot\mathbf{q} + \frac{\mathbf{J}\cdot\mathbf{J}}{\sigma} - \frac{\partial q_r}{\partial z} + \mu\phi, \tag{13}$$

where c is the specific heat, ϕ is the viscous dissipation, and q_r is the radiative heat flux. On the basis of the Rosseland approximation for radiation [42], q_r is defined as

$$q_r = -\frac{4\sigma^*}{3k^*}\frac{\partial T^4}{\partial z}, \tag{14}$$

in which σ^* and k^* are the Stefan-Boltzman constant and the absorption coefficient, respectively. Assuming that the temperature difference of fluid flow on the infinite plate is very small, which makes T^4 be expressed by the Taylor series expansion about T_∞ neglecting the higher-order term [39, 43], we have

$$T^4 = 4T_\infty T - 3T_\infty^4. \tag{15}$$

Combined Eqs. (12)-(15), the time fractional governing equation of the fluid temperature distribution with the Hall effect is obtained:

$$\begin{aligned} &\rho c\left(\frac{\partial T}{\partial t} + \tau_q^\gamma\, {}_0D_t^{1+\gamma} T\right) \\ &= \kappa\frac{\partial^2 T}{\partial z^2} + \frac{16\sigma^* T_\infty^3}{3k^*}\left(1 + \tau_q^\gamma\, {}_0D_t^\gamma\right)\frac{\partial^2 T}{\partial z^2} \\ &\quad + \frac{\sigma B_0^2}{1+m^2}\left(1 + \tau_q^\gamma\, {}_0D_t^\gamma\right)\left(u^2 + v^2\right) \\ &\quad + \mu\left(1 + \tau_q^\gamma\, {}_0D_t^\gamma\right)\left[\left(\frac{\partial u}{\partial z}\right)^2 + \left(\frac{\partial v}{\partial z}\right)^2\right]. \end{aligned} \tag{16}$$

The initial and boundary conditions of the fluid heat transfer are

$$\begin{aligned} t = 0 &: T(z,0) = T_\infty, \quad \frac{\partial T(z,0)}{\partial t} = 0, \\ t > 0 &: \begin{cases} T(0,t) = T_w, & z = 0, \\ T(z,t) = T_\infty, & z \to \infty. \end{cases} \end{aligned} \tag{17}$$

Define the following dimensionless variables:

$$\begin{aligned} &u^* = \frac{u}{U_0}, \quad v^* = \frac{v}{U_0}, \quad z^* = \frac{z}{H}, \quad t^* = \frac{\mu}{\rho H^2}t, \\ &\lambda^* = \frac{\mu}{\rho H^2}\lambda, \quad a^* = \frac{\rho H^2}{\mu}a, \quad \Omega^* = \frac{\rho H^2}{\mu}\Omega, \\ &\theta = \frac{T - T_\infty}{T_w - T_\infty}, \qquad Ha = HB_0\sqrt{\frac{\sigma}{\mu}}, \\ &Gr = \frac{\rho g\beta_T H^2(T_w - T_\infty)}{\mu U_0}, \quad Pr = \frac{\mu c}{\kappa}, \\ &Br = \frac{\mu U_0^2}{\kappa(T_w - T_\infty)}, \qquad R = \frac{16\sigma^* T_\infty^3}{3k^*\kappa}, \end{aligned} \tag{18}$$

where H is the characteristic length. Then, neglected the modified pressure gradient term in Eqs. (9) and (10), the dimensionless governing equations of the velocity field are established by using Eq. (18) (for brevity, the dimensionless mark "*" is omitted below),

$$\begin{aligned} &\frac{\partial u}{\partial t} + \int_0^1 \varpi(\alpha)\lambda^\alpha\, {}_0D_t^{1+\alpha} u\mathrm{d}\alpha \\ &+ \frac{Ha^2}{1+m^2}\left[u + \int_0^1 \varpi(\alpha)\lambda^\alpha\, {}_0D_t^\alpha u\mathrm{d}\alpha\right] \\ &- \left(2\Omega + \frac{mHa^2}{1+m^2}\right)\left[v + \int_0^1 \varpi(\alpha)\lambda^\alpha\, {}_0D_t^\alpha v\mathrm{d}\alpha\right] \\ &= \frac{\partial^2 u}{\partial z^2} + Gr\left[\theta + \int_0^1 \varpi(\alpha)\lambda^\alpha\, {}_0D_t^\alpha\theta\mathrm{d}\alpha\right], \end{aligned} \tag{19}$$

$$\begin{aligned}&\frac{\partial v}{\partial t}+\int_0^1 \varpi(\alpha)\lambda^{\alpha}\,{}_0D_t^{1+\alpha}v\mathrm{d}\alpha\\&+\frac{Ha^2}{1+m^2}\left[v+\int_0^1 \varpi(\alpha)\lambda^{\alpha}\,{}_0D_t^{\alpha}v\mathrm{d}\alpha\right]\\&+\left(2\Omega+\frac{mHa^2}{1+m^2}\right)\left[u+\int_0^1 \varpi(\alpha)\lambda^{\alpha}\,{}_0D_t^{\alpha}u\mathrm{d}\alpha\right]\\&=\frac{\partial^2 v}{\partial z^2}.\end{aligned}\tag{20}$$

If $\varpi(\alpha)=\delta(\alpha-\alpha_0)$, Eqs. (19) and (20) will be reduced to the flow system of fractional Maxwell fluid with the order α_0 [44]. And then, substituted Eq. (18) into Eq. (16), the dimensionless heat transfer equation is rearranged as

$$\begin{aligned}&\frac{\partial\theta}{\partial t}+\tau_q^{\gamma}\,{}_0D_t^{1+\gamma}\theta\\&=\frac{1}{Pr}\left[1+R(1+\tau_q^{\gamma}\,{}_0D_t^{\gamma})\right]\frac{\partial^2\theta}{\partial z^2}\\&\quad+\frac{Ha^2}{1+m^2}\frac{Br}{Pr}\left(1+\tau_q^{\gamma}\,{}_0D_t^{\gamma}\right)\left(u^2+v^2\right)\\&\quad+\frac{Br}{Pr}\left(1+\tau_q^{\gamma}\,{}_0D_t^{\gamma}\right)\left[\left(\frac{\partial u}{\partial z}\right)^2+\left(\frac{\partial v}{\partial z}\right)^2\right].\end{aligned}\tag{21}$$

The corresponding dimensionless initial and boundary conditions of velocity and temperature fields are

$$\begin{aligned}&t=0:\begin{cases}u(z,0)=0, & \dfrac{\partial u(z,0)}{\partial t}=0,\\ v(z,0)=0, & \dfrac{\partial v(z,0)}{\partial t}=0,\\ \theta(z,0)=0, & \dfrac{\partial\theta(z,0)}{\partial t}=0,\end{cases}\\&t>0:\begin{cases}u(0,t)=e^{-at}, & v(0,t)=0, \quad z=0,\\ u(z,t)\to 0, & v(z,t)\to 0, \quad z\to\infty,\\ \theta(0,t)=1, & z=0,\\ \theta(z,t)=0, & z\to\infty.\end{cases}\end{aligned}\tag{22}$$

3. Numerical solutions of the flow and heat transfer models

In order to study the MHD flow and heat transfer of generalized Maxwell fluid on a rotating infinite plate, the numerical solutions of the time fractional governing equations of velocity and temperature distributions are developed by the finite difference method. Firstly, we approximate the integral terms of the distributed order time fractional models Eqs. (19) and (20) based on the midpoint quadrature formula [45,46],

$$\begin{aligned}&\int_0^1 \varpi(\alpha)\lambda^{\alpha}\,{}_0D_t^{\alpha}\phi(z,t)\mathrm{d}\alpha\\&=\sum_{s=1}^{q}\varpi(\alpha_s)\lambda^{\alpha_s}\,{}_0D_t^{\alpha_s}\phi(z,t)\Delta\xi_s,\end{aligned}\tag{23}$$

$$\begin{aligned}&\int_0^1 \varpi(\alpha)\lambda^{\alpha}\,{}_0D_t^{1+\alpha}\psi(z,t)\mathrm{d}\alpha\\&=\sum_{s=1}^{q}\varpi(\alpha_s)\lambda^{\alpha_s}\,{}_0D_t^{1+\alpha_s}\psi(z,t)\Delta\xi_s,\end{aligned}\tag{24}$$

where $\phi=u,v,\theta$, $\psi=u,v$. Then Eqs. (19) and (20) can be arranged as

$$\begin{aligned}&\frac{\partial u(z,t)}{\partial t}+\sum_{s=1}^{q}d_s\,{}_0D_t^{1+\alpha_s}u(z,t)\\&+\frac{Ha^2}{1+m^2}\left(1+\sum_{s=1}^{q}d_s\,{}_0D_t^{\alpha_s}\right)u(z,t)\\&-\left(2\Omega+\frac{mHa^2}{1+m^2}\right)\left(1+\sum_{s=1}^{q}d_s\,{}_0D_t^{\alpha_s}\right)v(z,t)\\&=\frac{\partial^2 u(z,t)}{\partial z^2}+Gr\left(1+\sum_{s=1}^{q}d_s\,{}_0D_t^{\alpha_s}\right)\theta(z,t)+O(\varepsilon^2),\end{aligned}\tag{25}$$

$$\begin{aligned}&\frac{\partial v(z,t)}{\partial t}+\sum_{s=1}^{q}d_s\,{}_0D_t^{1+\alpha_s}v(z,t)\\&+\frac{Ha^2}{1+m^2}\left(1+\sum_{s=1}^{q}d_s\,{}_0D_t^{\alpha_s}\right)v(z,t)\\&+\left(2\Omega+\frac{mHa^2}{1+m^2}\right)\left(1+\sum_{s=1}^{q}d_s\,{}_0D_t^{\alpha_s}\right)u(z,t)\\&=\frac{\partial^2 v(z,t)}{\partial z^2}+O(\varepsilon^2),\end{aligned}\tag{26}$$

where $d_s=\varpi(\alpha_s)\lambda^{\alpha_s}\Delta\xi_s$, $\Delta\xi_s=\frac{1}{q}=\varepsilon$, and $\alpha_s=\frac{(s-1)\Delta\xi_s+s\Delta\xi_s}{2}=\frac{2s-1}{2q}$, $s=0,1,2,\cdots,q$.

For temporal and spatial variables, the intervals $[0,T_m]$ and $[0,L]$ are discretized into N and M equal subintervals, respectively. Take $t_n=n\tau$, $0\le n\le N$ and $z_i=ih$, $0\le i\le M$, where $\tau=T_m/N$ is the time step and $h=L/M$ is the space step. The grid functions u_i^n, v_i^n and θ_i^n are defined as the numerical solutions of $u(z,t)$, $v(z,t)$ and $\theta(z,t)$ at the mesh point (z_i,t_n), and the following notations are introduced:

$$\begin{aligned}&u_i^{n-\frac{1}{2}}=\frac{u_i^n+u_i^{n-1}}{2}, \quad v_i^{n-\frac{1}{2}}=\frac{v_i^n+v_i^{n-1}}{2},\\&\theta_i^{n-\frac{1}{2}}=\frac{\theta_i^n+\theta_i^{n-1}}{2}, \quad \delta_t u_i^{n-\frac{1}{2}}=\frac{u_i^n-u_i^{n-1}}{\tau},\\&\delta_t v_i^{n-\frac{1}{2}}=\frac{v_i^n-v_i^{n-1}}{\tau}, \ \delta_t\theta_i^{n-\frac{1}{2}}=\frac{\theta_i^n-\theta_i^{n-1}}{\tau}.\end{aligned}\tag{27}$$

For the Caputo fractional derivetive of $u(z_i,t_n)$ with order α_s $(0<\alpha_s<1)$, the L1 formula is presented as [47,48]

$$\begin{aligned}{}_0D_t^{\alpha_s}\psi(z_i,t_n)=\frac{\tau^{-\alpha_s}}{\Gamma(2-\alpha_s)}\Bigg[&a_0^{(\alpha_s)}\psi_i^n-\sum_{k=1}^{n-1}\Big(a_{n-k-1}^{(\alpha_s)}\\&-a_{n-k}^{(\alpha_s)}\Big)\psi_i^k-a_{n-1}^{(\alpha_s)}\psi_i^0\Bigg]+O(\tau^{2-\alpha_s}).\end{aligned}\tag{28}$$

Then, on the basis of Eq. (28), the approximational formula of the Caputo fractional derivative with order $1+\alpha_s$, $(1<1+\alpha_s<2)$ at the mesh points (z_i,t_n) and (z_i,t_{n-1}) are derived:

$$\begin{aligned}&\frac{1}{2}\left[{}_0D_t^{1+\alpha_s}\psi(z_i,t_n)+{}_0D_t^{1+\alpha_s}\psi(z_i,t_{n-1})\right]\\&={}_0D_t^{1+\alpha_s}\psi_i^{n-\frac{1}{2}}\\&=\frac{\tau^{-\alpha_s}}{\Gamma(2-\alpha_s)}\left[a_0^{(\alpha_s)}\delta_t\psi_i^{n-\frac{1}{2}}-\sum_{k=1}^{n-1}\left(a_{n-k-1}^{(\alpha_s)}\right.\right.\\&\left.\left.-a_{n-k}^{(\alpha_s)}\right)\delta_t\psi_i^{k-\frac{1}{2}}-a_{n-1}^{(\alpha_s)}\frac{\partial\psi(x_i,t_0)}{\partial t}\right]+O(\tau^{2-\alpha_s}),\end{aligned}\tag{29}$$

in which

$$a_l^{(\alpha_s)}=(l+1)^{1-\alpha_s}-l^{1-\alpha_s},\quad k=0,1,2,\cdots.\tag{30}$$

Similarly, the same discrete forms for the Caputo fractional derivative of $\theta(z_i,t_n)$ are given:

$$\begin{aligned}&{}_0D_t^{\gamma}\theta(z_i,t_n)\\&=\frac{\tau^{-\gamma}}{\Gamma(2-\gamma)}\left[a_0^{(\gamma)}\theta_i^n-\sum_{k=1}^{n-1}\left(a_{n-k-1}^{(\gamma)}\right.\right.\\&\left.\left.-a_{n-k}^{(\gamma)}\right)\theta_i^k-a_{n-1}^{(\gamma)}\theta_i^0\right]+O(\tau^{2-\gamma}),\ 0<\gamma<1,\end{aligned}\tag{31}$$

and

$$\begin{aligned}&\frac{1}{2}\left[{}_0D_t^{1+\gamma}\theta(z_i,t_n)+{}_0D_t^{1+\gamma}\theta(z_i,t_{n-1})\right]\\&={}_0D_t^{1+\alpha_s}\theta_i^{n-\frac{1}{2}}\\&=\frac{\tau^{-\gamma}}{\Gamma(2-\gamma)}\left[a_0^{(\gamma)}\delta_t\theta_i^{n-\frac{1}{2}}-\sum_{k=1}^{n-1}\left(a_{n-k-1}^{(\gamma)}\right.\right.\\&\left.\left.-a_{n-k}^{(\gamma)}\right)\delta_t\theta_i^{k-\frac{1}{2}}-a_{n-1}^{(\gamma)}\frac{\partial\theta(x_i,t_0)}{\partial t}\right]+O(\tau^{2-\gamma}).\end{aligned}\tag{32}$$

For the discretization of nonlinear terms of Eq. (21), the corresponding approximation formulas are considered,

$$\begin{aligned}&{}_0D_t^{\gamma}\left[\psi(z_i,t_n)\right]^2\\&=\frac{\tau^{-\gamma}}{\Gamma(2-\gamma)}\left[a_0^{(\gamma)}\left(\phi_i^n\right)^2-\sum_{k=1}^{n-1}\left(a_{n-k-1}^{(\gamma)}\right.\right.\\&\left.\left.-a_{n-k}^{(\gamma)}\right)\left(\phi_i^k\right)^2-a_{n-1}^{(\gamma)}\left(\phi_i^0\right)^2\right]+O(\tau^{2-\gamma}),\end{aligned}\tag{33}$$

and

$$\begin{aligned}&{}_0D_t^{\gamma}\left[\frac{\partial\psi(z_i,t_n)}{\partial z}\right]^2\\&=\frac{\tau^{-\gamma}}{\Gamma(2-\gamma)}\left[a_0^{(\gamma)}\left(\frac{\partial\psi(z_i,t_n)}{\partial z}\right)^2\right.\\&-\sum_{k=1}^{n-1}\left(a_{n-k-1}^{(\gamma)}-a_{n-k}^{(\gamma)}\right)\left(\frac{\partial\psi(z_i,t_k)}{\partial z}\right)^2\\&\left.-a_{n-1}^{(\gamma)}\left(\frac{\partial\psi(z_i,t_0)}{\partial z}\right)^2\right]+O(\tau^{2-\gamma}).\end{aligned}\tag{34}$$

For the integer order terms, the following difference formats are obtained by using the central differences:

$$\frac{1}{2}\left[\frac{\partial\phi(z_i,t_n)}{\partial t}+\frac{\partial\phi(z_i,t_{n-1})}{\partial t}\right]=\frac{\phi_i^n-\phi_i^{n-1}}{\tau}+O(\tau^2),\tag{35}$$

and

$$\begin{aligned}\frac{\partial^2\phi(z_i,t_n)}{\partial z^2}&=\frac{\phi_{i+1}^n-2\phi_i^n+\phi_{i-1}^n}{h^2}+O(h^2),\\\frac{\partial\psi(z_i,t_n)}{\partial z}&=\frac{\psi_{i+1}^n-\psi_{i-1}^n}{2h}+O(h^2).\end{aligned}\tag{36}$$

Then, define $I=\frac{mHa^2}{1+m^2}$, and $J=2\Omega+\frac{mHa^2}{1+m^2}$. The governing equations of the velocity distributions by averaging Eqs. (25) and (26) at grid points (z_i,t_n) and (z_i,t_{n-1}) are shown as

$$\begin{aligned}&\frac{1}{2}\left[\frac{\partial u(z_i,t_n)}{\partial t}+\frac{\partial u(z_i,t_{n-1})}{\partial t}\right]\\&+\frac{1}{2}\sum_{s=1}^{q}d_s\,{}_0D_t^{1+\alpha_s}\left[u(z_i,t_n)+u(z_i,t_{n-1})\right]\\&+\frac{1}{2}I\left(1+\sum_{s=1}^{q}d_s\,{}_0D_t^{\alpha_s}\right)\left[u(z_i,t_n)+u(z_i,t_{n-1})\right]\\&-\frac{1}{2}J\left(1+\sum_{s=1}^{q}d_s\,{}_0D_t^{\alpha_s}\right)\left[v(z_i,t_n)+v(z_i,t_{n-1})\right]\\&=\frac{1}{2}\left[\frac{\partial^2u(z_i,t_{n-1})}{\partial z^2}+\frac{\partial^2u(z_i,t_{n-1})}{\partial z^2}\right]\\&+\frac{1}{2}Gr\left(1+\sum_{s=1}^{q}d_s\,{}_0D_t^{\alpha_s}\right)\left[\theta(z_i,t_n)+\theta(z_i,t_{n-1})\right]+O(\varepsilon^2),\end{aligned}\tag{37}$$

$$\begin{aligned}&\frac{1}{2}\left[\frac{\partial v(z_i,t_n)}{\partial t}+\frac{\partial v(z_i,t_{n-1})}{\partial t}\right]\\&+\frac{1}{2}\sum_{s=1}^{q}d_s\,{}_0D_t^{1+\alpha_s}\left[v(z_i,t_n)+v(z_i,t_{n-1})\right]\\&+\frac{1}{2}I\left(1+\sum_{s=1}^{q}d_s\,{}_0D_t^{\alpha_s}\right)\left[v(z_i,t_n)+v(z_i,t_{n-1})\right]\\&+\frac{1}{2}J\left(1+\sum_{s=1}^{q}d_s\,{}_0D_t^{\alpha_s}\right)\left[u(z_i,t_n)+u(z_i,t_{n-1})\right]\\&=\frac{1}{2}\left[\frac{\partial^2v(z_i,t_{n-1})}{\partial z^2}+\frac{\partial^2v(z_i,t_{n-1})}{\partial z^2}\right]+O(\varepsilon^2).\end{aligned}\tag{38}$$

Moreover, the nonlinear terms of Eq. (21) at the mesh point (z_i, t_n) are explicitly treated as

$$\begin{aligned}
&\frac{\partial\theta(z_i,t_n)}{\partial t}+\tau_q^\gamma\,{}_0D_t^{1+\gamma}\theta(z_i,t_n)\\
&=\frac{1}{Pr}\left[1+R(1+\tau_q^\gamma\,{}_0D_t^\gamma)\right]\frac{\partial^2\theta(z_i,t_n)}{\partial z^2}\\
&\quad+I\frac{Br}{Pr}(1+\tau_q^\gamma\,{}_0D_t^\gamma)\left[u(z_i,t_{n-1})\right]^2\\
&\quad+I\frac{Br}{Pr}(1+\tau_q^\gamma\,{}_0D_t^\gamma)\left[v(z_i,t_{n-1})\right]^2\\
&\quad+\frac{Br}{Pr}(1+\tau_q^\gamma\,{}_0D_t^\gamma)\left[\frac{\partial u(z_i,t_{n-1})}{\partial z}\right]^2\\
&\quad+\frac{Br}{Pr}(1+\tau_q^\gamma\,{}_0D_t^\gamma)\left[\frac{\partial v(z_i,t_{n-1})}{\partial z}\right]^2,
\end{aligned}\tag{39}$$

but the nonlinear terms at the mesh point (z_i, t_{n-1}) are handled implicitly and followed as

$$\begin{aligned}
&\frac{\partial\theta(z_i,t_{n-1})}{\partial t}+\tau_q^\gamma\,{}_0D_t^{1+\gamma}\theta(z_i,t_{n-1})\\
&=\frac{1}{Pr}\left[1+R(1+\tau_q^\gamma\,{}_0D_t^\gamma)\right]\frac{\partial^2\theta(z_i,t_{n-1})}{\partial z^2}\\
&\quad+I\frac{Br}{Pr}(1+\tau_q^\gamma\,{}_0D_t^\gamma)\left\{\left[u(z_i,t_{n-1})\right]^2+\left[v(z_i,t_{n-1})\right]^2\right\}\\
&\quad+I\frac{Br}{Pr}(1+\tau_q^\gamma\,{}_0D_t^\gamma)\left[v(z_i,t_{n-1})\right]^2\\
&\quad+\frac{Br}{Pr}(1+\tau_q^\gamma\,{}_0D_t^\gamma)\left[\frac{\partial u(z_i,t_{n-1})}{\partial z}\right]^2\\
&\quad+\frac{Br}{Pr}(1+\tau_q^\gamma\,{}_0D_t^\gamma)+\left[\frac{\partial v(z_i,t_{n-1})}{\partial z}\right]^2.
\end{aligned}\tag{40}$$

Then, we obtain

$$\begin{aligned}
&\frac{1}{2}\left[\frac{\partial\theta(z_i,t_n)}{\partial t}+\frac{\partial\theta(z_i,t_{n-1})}{\partial t}\right]\\
&+\frac{1}{2}\tau_q^\gamma\left[{}_0D_t^{1+\gamma}\theta(z_i,t_n)+{}_0D_t^{1+\gamma}\theta(z_i,t_{n-1})\right]\\
&=\frac{1}{2}\frac{1}{Pr}\left[1+R(1+\tau_q^\gamma\,{}_0D_t^\gamma)\right]\frac{\partial^2\theta(z_i,t_n)}{\partial z^2}\\
&\quad+\frac{1}{2}\frac{1}{Pr}\left[1+R(1+\tau_q^\gamma\,{}_0D_t^\gamma)\right]\frac{\partial^2\theta(z_i,t_{n-1})}{\partial z^2}\\
&\quad+\frac{Ha^2}{1+m^2}\frac{Br}{Pr}\left(1+\tau_q^\gamma\,{}_0D_t^\gamma\right)\left[u(z_i,t_{n-1})\right]^2\\
&\quad+\frac{Ha^2}{1+m^2}\frac{Br}{Pr}\left(1+\tau_q^\gamma\,{}_0D_t^\gamma\right)+\left[v(z_i,t_{n-1})\right]^2\\
&\quad+\frac{Br}{Pr}\left(1+\tau_q^\gamma\,{}_0D_t^\gamma\right)\left[\frac{\partial u(z_i,t_{n-1})}{\partial z}\right]^2\\
&\quad+\frac{Br}{Pr}\left(1+\tau_q^\gamma\,{}_0D_t^\gamma\right)\left[\frac{\partial v(z_i,t_{n-1})}{\partial z}\right]^2.
\end{aligned}\tag{41}$$

Finally, defining

$$P_s=d_s\frac{\tau^{-\alpha_s}}{\Gamma(2-\alpha_s)},\quad R_\gamma=\tau_q^\gamma\frac{\tau^{-\gamma}}{\Gamma(2-\gamma)},\tag{42}$$

and disregarding the error terms, the Crank-Nicolson finite difference schemes of multinomial time fractional governing Eqs. (37), (38) and (41) are presented based on Eqs. (27)-(35) and (50),

$$\begin{aligned}
&\frac{u_i^n-u_i^{n-1}}{\tau}+\sum_{s=1}^{q}P_s\left[a_0^{(\alpha_s)}\delta_t u_i^{n-\frac{1}{2}}\right.\\
&\left.-\sum_{k=1}^{n-1}\left(a_{n-k-1}^{(\alpha_s)}-a_{n-k}^{(\alpha_s)}\right)\delta_t u_i^{k-\frac{1}{2}}\right]\\
&+I\left(1+\sum_{s=1}^{q}P_s a_0^{(\alpha_s)}\right)\left(u_i^n+u_i^{n-1}\right)\\
&-I\sum_{s=1}^{q}P_s\sum_{k=1}^{n-1}\left(a_{n-k-1}^{(\alpha_s)}-a_{n-k}^{(\alpha_s)}\right)\left(u_i^k+u_i^{k-1}\right)\\
&-\frac{1}{2}J\left(1+\sum_{s=1}^{q}P_s a_0^{(\alpha_s)}\right)\left(v_i^n+v_i^{n-1}\right)\\
&+\frac{1}{2}J\sum_{s=1}^{q}P_s\sum_{k=1}^{n-1}\left(a_{n-k-1}^{(\alpha_s)}-a_{n-k}^{(\alpha_s)}\right)\left(v_i^k+v_i^{k-1}\right)\\
&=\frac{1}{2}\left(\frac{u_{i+1}^n-2u_i^n+u_{i-1}^n}{h^2}+\frac{u_{i+1}^{n-1}-2u_i^{n-1}+u_{i-1}^{n-1}}{h^2}\right)\\
&\quad+\frac{Gr}{2}\left(1+\sum_{s=1}^{q}P_s a_0^{(\alpha_s)}\right)\left(\theta_i^n+\theta_i^{n-1}\right)\\
&\quad-\frac{Gr}{2}\sum_{s=1}^{q}P_s\sum_{k=1}^{n-1}\left(a_{n-k-1}^{(\alpha_s)}-a_{n-k}^{(\alpha_s)}\right)\left(\theta_i^k+\theta_i^{k-1}\right),
\end{aligned}\tag{43}$$

$1\le n\le N,\ 1\le i\le M-1,$

$$\begin{aligned}
&\frac{v_i^n-v_i^{n-1}}{\tau}+\sum_{s=1}^{q}P_s\left[a_0^{(\alpha_s)}\delta_t v_i^{n-\frac{1}{2}}-\sum_{k=1}^{n-1}\left(a_{n-k-1}^{(\alpha_s)}\right.\right.\\
&\left.\left.-a_{n-k}^{(\alpha_s)}\right)\delta_t v_i^{k-\frac{1}{2}}\right]+I\left(1+\sum_{s=1}^{q}P_s a_0^{(\alpha_s)}\right)\left(v_i^n+v_i^{n-1}\right)\\
&-I\sum_{s=1}^{q}P_s\sum_{k=1}^{n-1}\left(a_{n-k-1}^{(\alpha_s)}-a_{n-k}^{(\alpha_s)}\right)\left(v_i^k+v_i^{k-1}\right)\\
&+\frac{1}{2}J\left(1+\sum_{s=1}^{q}P_s a_0^{(\alpha_s)}\right)\left(u_i^n+u_i^{n-1}\right)\\
&-\frac{1}{2}J\sum_{s=1}^{q}P_s\sum_{k=1}^{n-1}\left(a_{n-k-1}^{(\alpha_s)}-a_{n-k}^{(\alpha_s)}\right)\left(u_i^k+u_i^{k-1}\right)\\
&=\frac{1}{2}\left(\frac{u_{i+1}^n-2u_i^n+u_{i-1}^n}{h^2}+\frac{u_{i+1}^{n-1}-2u_i^{n-1}+u_{i-1}^{n-1}}{h^2}\right),
\end{aligned}\tag{44}$$

$1\le n\le N,\ 1\le i\le M-1,$

$$\begin{aligned}
&\frac{\theta_i^n-\theta_i^{n-1}}{\tau}\\
&+R_\gamma\left[a_0^{(\gamma)}\delta_t\theta_i^{n-\frac{1}{2}}-\sum_{k=1}^{n-1}\left(a_{n-k-1}^{(\gamma)}-a_{n-k}^{(\gamma)}\right)\delta_t\theta_i^{k-\frac{1}{2}}\right]
\end{aligned}$$

$$
\begin{aligned}
&= \frac{1}{2Pr}\left[1+R\left(1+R_\gamma a_0^{(\gamma)}\right)\right]\left(\frac{\theta_{i+1}^n-2\theta_i^n+\theta_{i-1}^n}{h^2}\right.\\
&\left.+\frac{\theta_{i+1}^{n-1}-2\theta_i^{n-1}+\theta_{i-1}^{n-1}}{h^2}\right)\\
&-\frac{R}{2Pr}R_\gamma\sum_{k=1}^{n-1}\left(a_{n-k-1}^{(\gamma)}-a_{n-k}^{(\gamma)}\right)\left(\frac{\theta_{i+1}^k-2\theta_i^k+\theta_{i-1}^k}{h^2}\right.\\
&\left.+\frac{\theta_{i+1}^{k-1}-2\theta_i^{k-1}+\theta_{i-1}^{k-1}}{h^2}\right)\\
&+I\frac{Br}{Pr}\left(1+R_\gamma a_0^{(\gamma)}\right)\left[(u_i^{n-1})^2+(v_i^{n-1})^2\right]\\
&-I\frac{Br}{Pr}R_\gamma\sum_{k=1}^{n-2}\left(a_{n-k-2}^{(\gamma)}-a_{n-k-1}^{(\gamma)}\right)\left[(u_i^k)^2+(v_i^k)^2\right]\\
&+\frac{Br}{Pr}\left(1+R_\gamma a_0^{(\gamma)}\right)\left[\left(\frac{u_{i+1}^{n-1}-u_{i-1}^{n-1}}{2h}\right)^2\right.\\
&\left.+\left(\frac{v_{i+1}^{n-1}-v_{i-1}^{n-1}}{2h}\right)^2\right]\\
&-\frac{Br}{Pr}R_\gamma\sum_{k=1}^{n-2}\left(a_{n-k-2}^{(\gamma)}-a_{n-k-1}^{(\gamma)}\right)\left[\left(\frac{u_{i+1}^{k}-u_{i-1}^{k}}{2h}\right)^2\right.\\
&\left.+\left(\frac{v_{i+1}^{k}-v_{i-1}^{k}}{2h}\right)^2\right],\quad 1\le n\le N,\ 1\le i\le M-1.
\end{aligned}
\tag{45}
$$

The initial and boundary conditions Eq. (50) can be discretized as

$$
\begin{aligned}
&u_i^0=0,\quad v_i^0=0,\quad \theta_i^0=0,\quad n=0,\ 0\le i\le M,\\
&r_i^0=0,\quad p_i^0=0,\quad \phi_i^0=0,\quad n=0,\ 0\le i\le M,\\
&u_0^n=e^{-an\tau},\ v_0^n=0,\ \theta_0^n=1,\quad 1\le n\le N,\ i=0,\\
&u_M^n\to 0,\ v_M^n\to 0,\ \theta_M^n=0,\quad 1\le n\le N,\ i=M.
\end{aligned}
\tag{46}
$$

Thus, the numerical solutions of governing equations for velocities and temperature are obtained based on the above difference schemes Eqs. (43)-(46).

4. Numerical example

In order to check the effectiveness of the finite difference schemes, the following coupled, fractional partial differential equations with exact solutions are given:

$$
\begin{aligned}
&\frac{\partial u}{\partial t}+\int_0^1\varpi(\alpha)\lambda^\alpha\,{}_0D_t^{1+\alpha}u\mathrm{d}\alpha\\
&+\frac{Ha^2}{1+m^2}\left[u+\int_0^1\varpi(\alpha)\lambda^\alpha\,{}_0D_t^\alpha u\mathrm{d}\alpha\right]\\
&-\left(2\Omega+\frac{mHa^2}{1+m^2}\right)\left[v+\int_0^1\varpi(\alpha)\lambda^\alpha\,{}_0D_t^\alpha v\mathrm{d}\alpha\right]\\
&=\frac{\partial^2 u}{\partial z^2}+Gr\left[\theta+\int_0^1\varpi(\alpha)\lambda^\alpha\,{}_0D_t^\alpha\theta\mathrm{d}\alpha\right]+f_1,\\
&\frac{\partial v}{\partial t}+\int_0^1\varpi(\alpha)\lambda^\alpha\,{}_0D_t^{1+\alpha}v\mathrm{d}\alpha\\
&+\frac{Ha^2}{1+m^2}\left[v+\int_0^1\varpi(\alpha)\lambda^\alpha\,{}_0D_t^\alpha v\mathrm{d}\alpha\right]\\
&+\left(2\Omega+\frac{mHa^2}{1+m^2}\right)\left[u+\int_0^1\varpi(\alpha)\lambda^\alpha\,{}_0D_t^\alpha u\mathrm{d}\alpha\right]\\
&=\frac{\partial^2 v}{\partial z^2}+f_2,
\end{aligned}
\tag{48}
$$

$$
\begin{aligned}
&\frac{\partial\theta}{\partial t}+\tau_q^\gamma\,{}_0D_t^{1+\gamma}\theta\\
&=\frac{1}{Pr}\left[1+R(1+\tau_q^\gamma\,{}_0D_t^\gamma)\right]\frac{\partial^2\theta}{\partial z^2}\\
&+\frac{Ha^2}{1+m^2}\frac{Br}{Pr}\left(1+\tau_q^\gamma\,{}_0D_t^\gamma\right)\left(u^2+v^2\right)\\
&+\frac{Br}{Pr}\left(1+\tau_q^\gamma\,{}_0D_t^\gamma\right)\left[\left(\frac{\partial u}{\partial z}\right)^2+\left(\frac{\partial v}{\partial z}\right)^2\right]+f_3,
\end{aligned}
\tag{49}
$$

and the initial and boundary conditions are satisfied:

$$
\begin{aligned}
&t=0:\begin{cases}u(z,0)=0, & \dfrac{\partial u(z,0)}{\partial t}=0,\\ v(z,0)=0, & \dfrac{\partial v(z,0)}{\partial t}=0,\\ \theta(z,0)=0, & \dfrac{\partial\theta(z,0)}{\partial t}=0,\end{cases}\\
&t>0:\begin{cases}u(0,t)=0, & v(0,t)=0,\ z=0,\\ u(z,t)=0, & v(z,t)=0,\ z=L,\\ \theta(0,t)=0, & z=0,\\ \theta(z,t)=0, & z=L,\end{cases}
\end{aligned}
\tag{50}
$$

where f_1, f_2 and f_3 refer to the source terms of z and t, and are defined as

$$
\begin{aligned}
&f_1(z,t)\\
&=2t^2+2tz(L-z)\\
&+z(L-z)\int_0^1\varpi(\alpha)\lambda^\alpha\,{}_0D_t^{1+\alpha}t^2\mathrm{d}\alpha\\
&+\frac{Ha^2}{1+m^2}z(L-z)\left[t^2+\int_0^1\varpi(\alpha)\lambda^\alpha\,{}_0D_t^\alpha t^2\mathrm{d}\alpha\right]\\
&-\left(2\Omega+\frac{mHa^2}{1+m^2}\right)z(L-z)^2\left[t^3+\int_0^1\varpi(\alpha)\lambda^\alpha\,{}_0D_t^\alpha t^3\mathrm{d}\alpha\right]\\
&-3Grz^2(L-z)\left[t^2+\int_0^1\varpi(\alpha)\lambda^\alpha\,{}_0D_t^\alpha t^2\mathrm{d}\alpha\right],\\
&f_2(z,t)\\
&=-t^3(-4L+6z)+3t^2z(L-z)^2\\
&+z(L-z)^2\int_0^1\varpi(\alpha)\lambda^\alpha\,{}_0D_t^{1+\alpha}t^3\mathrm{d}\alpha\\
&+\frac{Ha^2}{1+m^2}z(L-z)^2\left[t^3+\int_0^1\varpi(\alpha)\lambda^\alpha\,{}_0D_t^\alpha t^3\mathrm{d}\alpha\right]
\end{aligned}
\tag{51}
$$

$$-\left(2\Omega+\frac{mHa^2}{1+m^2}\right)z(L-z)\left[t^2+\int_0^1 \varpi(\alpha)\lambda^{\alpha}\,{}_0D_t^{\alpha}t^2\mathrm{d}\alpha\right], \tag{52}$$

$$\begin{aligned} f_3(z,t) &= z^2(L-z)\left(6t+3\tau_q^{\gamma}\,{}_0D_t^{1+\gamma}t^2\right) \\ &\quad -\frac{6}{Pr}(L-3z)\left[1+R\left(1+\tau_q^{\gamma}\,{}_0D_t^{\gamma}\right)\right]t^2 \\ &\quad -\frac{Ha^2}{1+m^2}\frac{Br}{Pr}z^2(L-z)^2\left(1+\tau_q^{\gamma}\,{}_0D_t^{\gamma}\right)t^4 \\ &\quad -\frac{Ha^2}{1+m^2}\frac{Br}{Pr}z^2(L-z)^4\left(1+\tau_q^{\gamma}\,{}_0D_t^{\gamma}\right)t^6 \\ &\quad -\frac{Br}{Pr}(L-2z)^2\left(1+\tau_q^{\gamma}\,{}_0D_t^{\gamma}\right)t^4 \\ &\quad +\frac{Br}{Pr}(L-z)^2(L-3z)^2\left(1+\tau_q^{\gamma}\,{}_0D_t^{\gamma}\right)t^6. \end{aligned} \tag{53}$$

The exact solutions of the system are $u(z,t)=t^2z(L-z)$, $v(z,t)=t^3z(L-z)^2$ and $\theta(z,t)=3t^2z^2(L-z)$.

And then, a comparison is made to prove the feasibility of numerical methods when $\varpi(\alpha)=2\alpha$, $\tau=1/200$, $h=1/100$, $\lambda=0.1$, $\Omega=0.5$, $\gamma=0.9$, $\tau_q=0.5$, $Pr=0.5$, $Br=0.15$, $Ha=0.15$, $Gr=0.1$, $R=1$, $a=1$ and $m=1$. Figure 2 shows the numerical and exact solutions of the fractional system. It is clearly that there is a high degree of consistency between the numerical solution and the exact solution, which indicates that the error between the numerical solution and the exact solution is minimal, demonstrating the effectiveness of the numerical method.

5. Results and discussion

In this section, the velocity and temperature distributions of the generalized Maxwell fluid charactered by the time distributed order fractional derivatives are investigated. In order to quantitatively analyze the flow velocity of the fluid, the weighted functions $\varpi(\alpha)$ for Eqs. (19) and (20) are considered to follow the power law distribution, i.e., $\varpi(\alpha)=\nu\alpha^{\nu-1}$, which is used to describe some physical phenomena followed by the ultraslow kinetics [44, 49]. Here, a linear increasing case is considered by taking $\nu=2$. For the heat transfer in fluid flow, the fractional energy equation (21) is constructed, which can be regarded as a special case of the distributed order fractional energy equation. This is because the distributed order fractional model can be reduced to the fractional model with the order γ_0 when the weight function obeys the Dirac delta function [44], i.e., $\delta(\gamma-\gamma_0)$. To accurately portray the flow and heat transfer characteristics of the fluid, some model parameters need to be determined. The governing equations of velocities and temperature are treated on the computational region $[0,2]$. The rest parameters have been provided in Sect. 4. Then, the effectiveness of the numerical method and the effects of some relevant parameters on fluid velocity and temperature distributions are studied at $t=0.5$. The results are shown in Figs. 3-9.

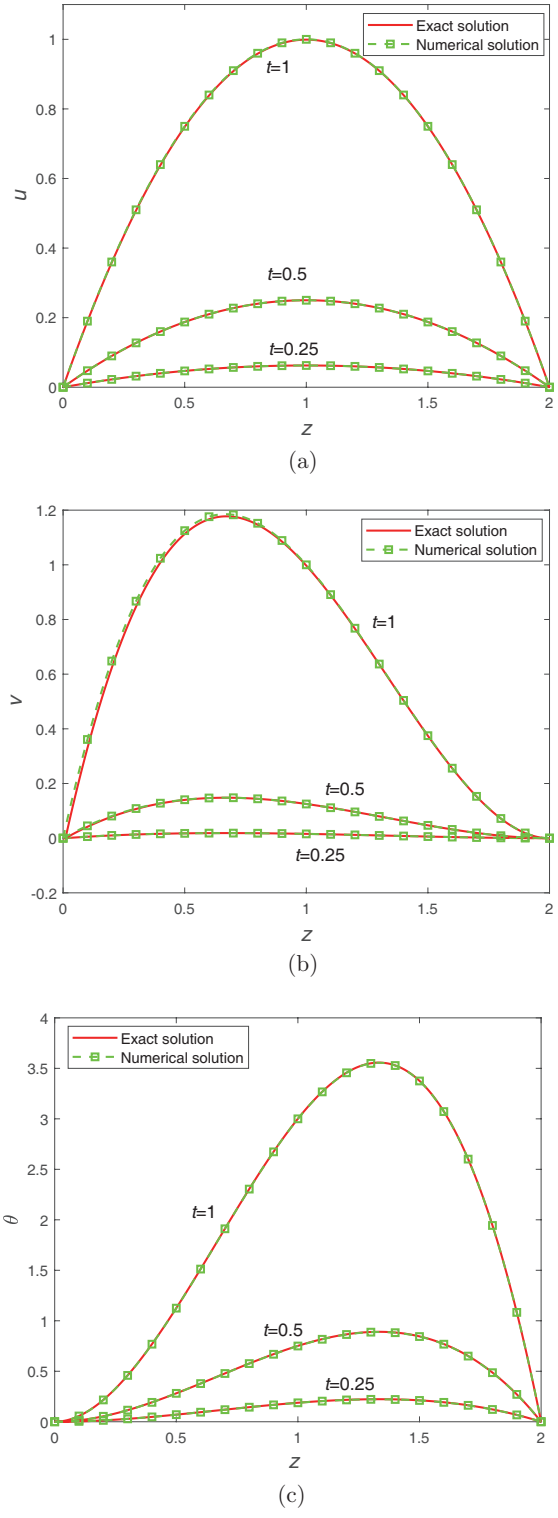

Figure 2 Comparison between numerical and exact solutions of the example.

5.1 Effectiveness of the numerical method

To verify the effectiveness and stability of the numerical method proposed above, we investigate the numerical solutions of the momentum and energy equations through the finite difference schemes. As shown in Fig. 3, we plot the velocities and temperature profiles by taking different N for $h = 1/100$ and M for $\tau = 1/200$, respectively. Obviously, when the space or time step is changed and the other variables are fixed, the values of u, v and θ are relatively stable

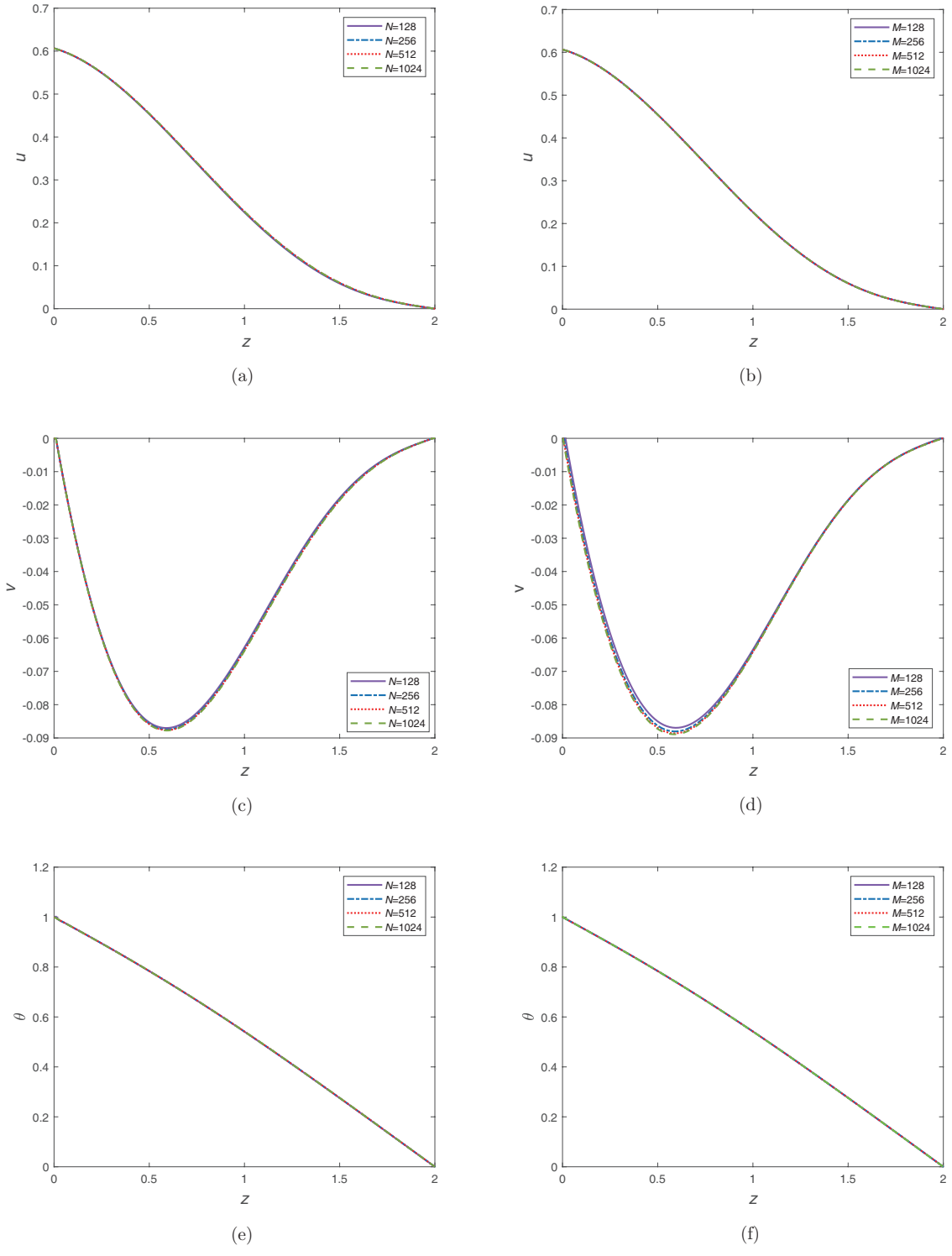

Figure 3 Numerical solutions of velocities and temperatures for different values of N and M.

and have no significant differences. The high consistencies of numerical solutions also indicate that the numerical method is effective and feasible in describing the unsteady MHD flow and heat transfer of complex viscoelastic fluid.

5.2 Effects of pertinent parameters on velocity distributions

It is well known that model parameters have important effects on the flow and heat teansfer processes of non-Newtonian fluids [50, 51]. Thus, in order to further study the flow properties of generalized Maxwell fluid with distributed order characteristics in rotating system, we present the influences of several pertinent parameters on fluid flow velocities u and v, graphically. As shown in Figs. 4-8, velocity profiles with z are drawn by considering different values of the relaxation time λ, rotational angular velocity Ω, Hartmann number Ha, thermal Grashof number Gr and Hall parameter m, respectively.

In Fig. 4, the velocity profiles with z are plotted. It is apparent that the flow velocities u and v show different fluctuation trends with λ. The increasing of λ leads to the steady velocities closer to the plate, which presents the phenomenon of heavy tail. It indicates the stress relaxation characteristics of the generalized Maxwell fluid model with power law weight function. Moreover, it is worth noting that the maximum values of velocity in the whole calculation area increase with the increase of λ. Then, for different Ω, the velocity distributions are given in Fig. 5. It can be found that the variations of Ω make the profiles of velocities u and v show a contrary regular. That is, as Ω increases, u decreases and v increases. It shows that the fluid deflection force caused by the rotation effect plays an important role in the velocity distributions.

In Fig. 6, the effects of Hartmann number Ha on velocities

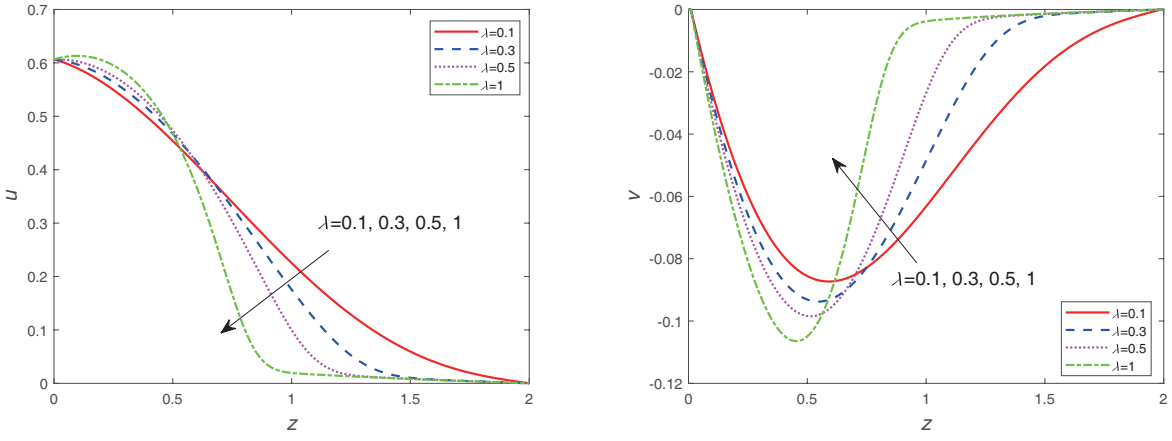

Figure 4 Velocity profiles of u and v for different λ.

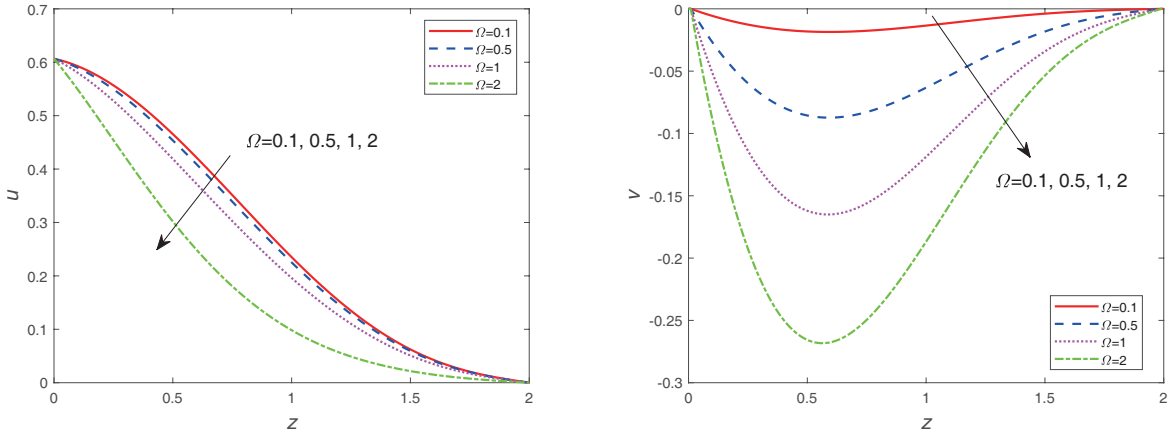

Figure 5 Velocity profiles of u and v for different Ω.

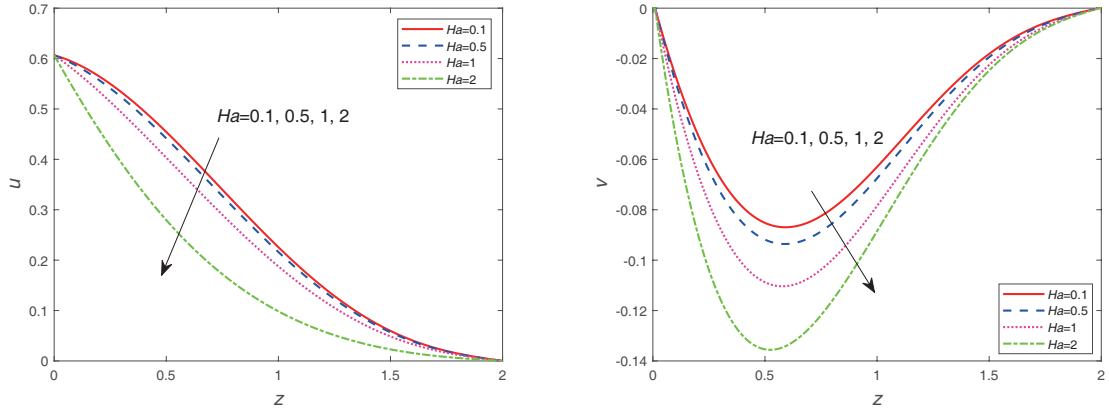

Figure 6 Velocity profiles of u and v for different Ha.

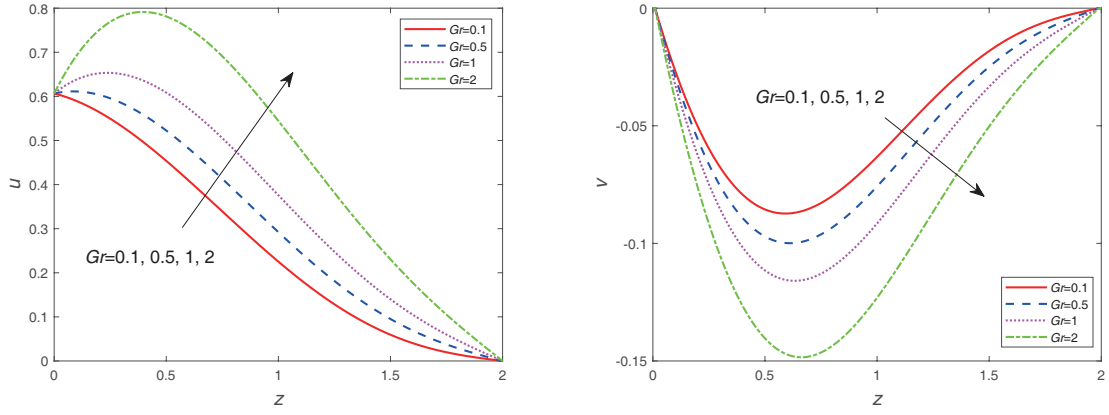

Figure 7 Velocity profiles of u and v for different Gr.

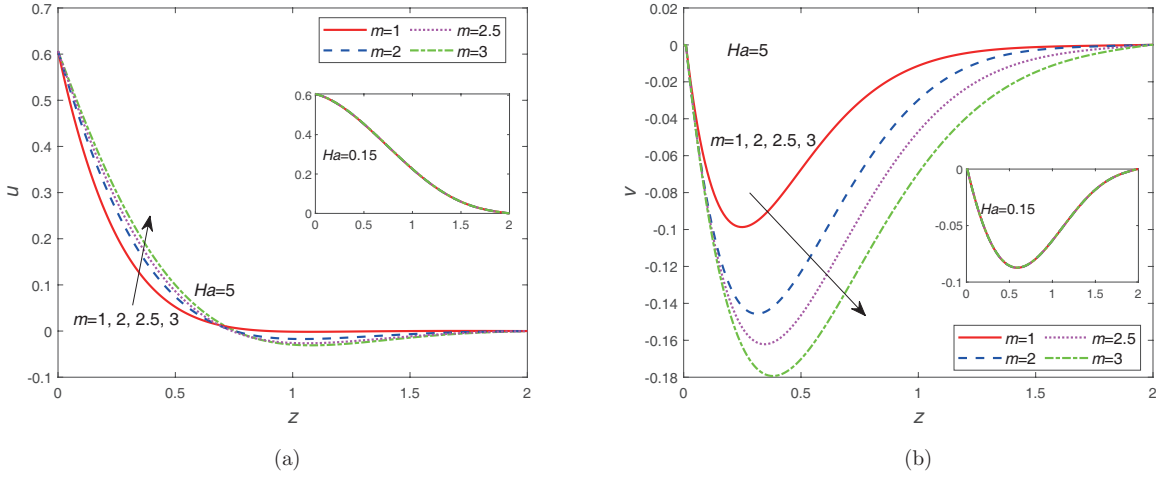

Figure 8 Velocity profiles of u and v for different m.

u and v are depicted. In the whole calculation region, we can see that the value of u decreases monotonically with z, but the value of v presents an analogous parabola characteristic. This is because the left boundary values of velocity u and v are different, which makes their velocity curves present different change rules. It indicates that the flow characteristics

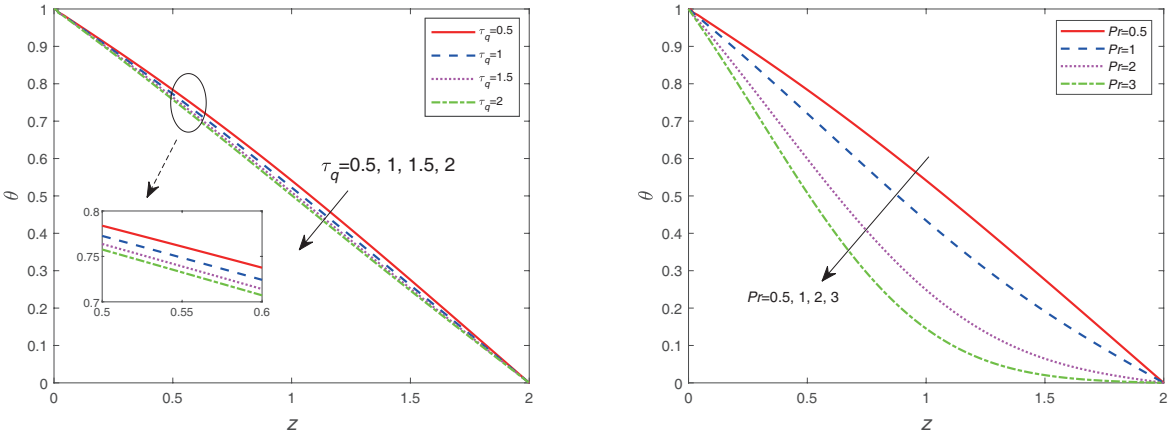

Figure 9 Temperature distributions for different τ_q and Pr.

of fluid at the boundary have a significant impact on the flow behavior in the whole region. Another obvious phenomenon is that Ha plays an important role in velocity distributions. We note that u reduces with the increase of Ha, and v raises in the wake of increase of Ha. It shows that the increase of Hartmann number means that the role of viscous force is relatively small, and the Lorentz force caused by the magnetic field acting on the fluid plays a leading role, but it will hinder the flow of the fluid [43]. Figure 7 plots the effect of thermal Grashof number on the fluid velocities. It is observed that due to the increase of Gr, the velocity distributions will fluctuate over the whole region. The values of the velocities u and v increase with the increase of Gr. And the greater Gr, the greater the maximum values of the velocities u and v. As shown in Fig. 8, the velocities profiles for different values of Hall parameter m are plotted. It is clear that when the magnetic field strength is weak, the flow velocity of the fluid is not affected by m, and when the magnetic field is strong, the fluid velocity changes with m. It shows that Hall effect has no significant effect on the velocities under the action of weakly magnetic field. In addition, it can be observed that a larger velocity components u and v are obtained with the increase of m in the presence of the strong magnetic field ($Ha = 5$), which indicates that the strong Hall effect plays an important role in the axial velocity distribution of the fluid.

5.3 Effects of pertinent parameters on temperature distributions

The effects of pertinent parameters on temperature distributions of the generalized Maxwell fluid are investigated. The temperature profiles for different values of relaxation time τ_q of the fractional heat conduction equation (21) are presented in Fig. 9(a). It can be seen that the increase of τ_q leads to the decrease of the temperature. The influences of the Prandtl number Pr on temperature of the fluid are depicted in Fig. 9(b). We note that temperature reduces with the increase of Pr. An important point is that Prandtl number can be used to describe the interaction between of momentum boundary layer and temperature boundary layer. The increase of Pr suggests that the fluid viscosity is raising and the thickening of momentum boundary layer is obtained, which leads to the decrease of thermal conductivity and the thinning of temperature boundary layer [43].

Figure 10(a) exhibits the temperature distributions of the generalized Maxwell fluid with the radiative heat flux for different values of R. The increase of radiation number R reduces the temperature of the fluid. It shows that the temperature curve is not only related to thermal radiation, but also affected by the heat transfer performance of fluid particles. For the different values of Brinkman number Br, the temperature profiles are plotted in Fig. 10(b). It can be found that the temperature raises with the addition of Br. The Brinkman number is used to depict the ratio between viscous effect and external heating of the flow. The large value of Br indicates that the viscous heat effect plays a dominant role in the process of heat conduction. When the viscosity heat effect is relatively strong, the heat transfer coefficient is relatively low and the temperature drop is relatively small. Finally, the effects of Hartmann number Ha and Hall parameter m on temperature distributions are given in Fig. 11. It is clear that the temperature profiles show a high degree of consistency when Ha takes different values. It suggests that the temperature is insensitive to changes of the external magnetic field. From Fig. 11(b), we notice that under the action of strong or weak magnetic field ($Ha = 5$ or $Ha = 0.15$), the influence of Hall parameter on temperature is extremely subtle. It is because the magnetic field and Hall effect directly affect the flow of

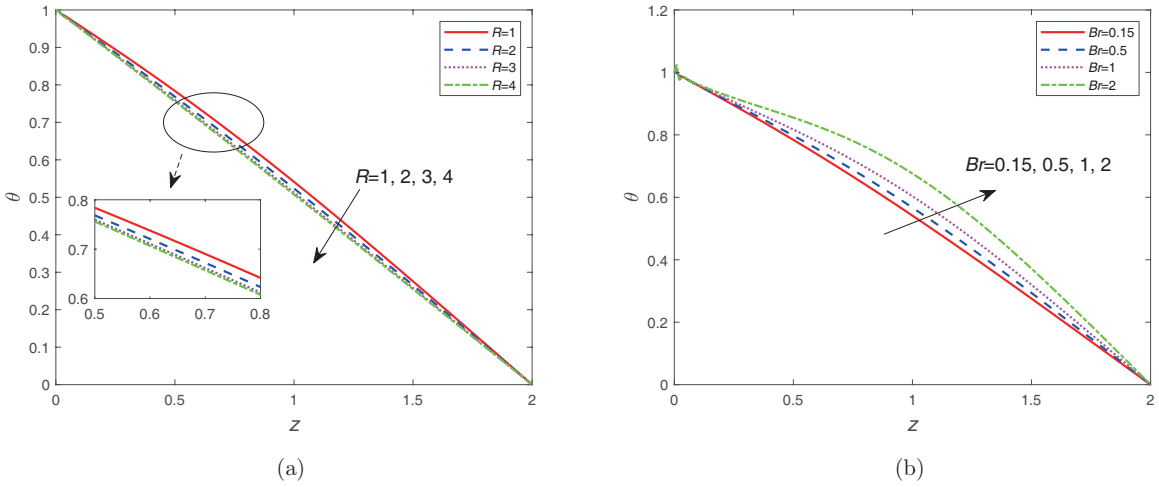

Figure 10 Temperature profiles for different R and Br.

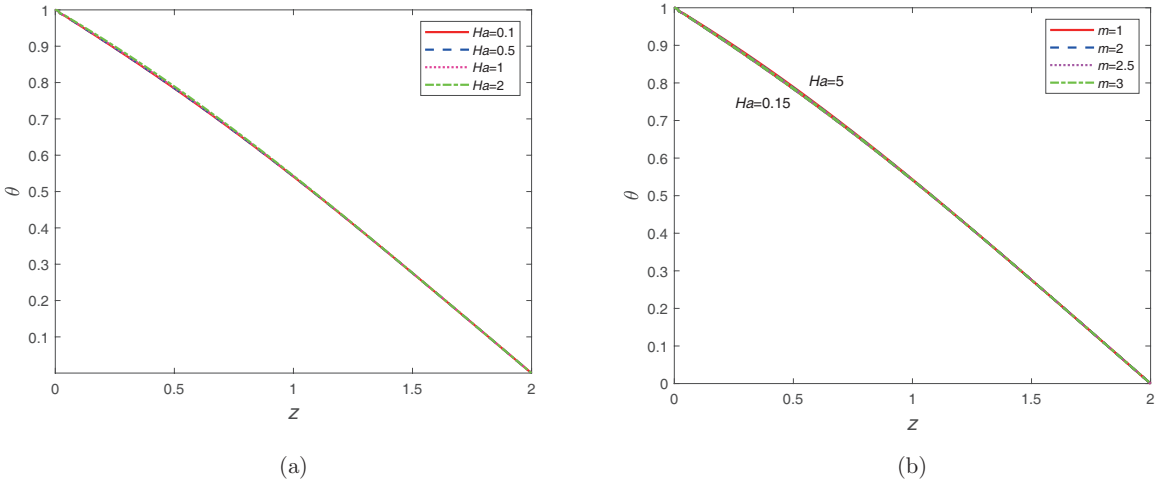

Figure 11 Temperature profiles for different Ha and m.

the fluid, and act on the temperature through the coupling effect.

6. Conclusions

In this work, we investigate the fractional models of the unsteady rotating MHD flow and heat transfer of generalized Maxwell fluid over an infinite plate in the presence of a strong magnetic field. Firstly, in view of the complexity of generalized Maxwell fluid flow and heat transfer, fractional calculus theory is introduced to depict the laws of the fluid motion and heat conduction, which deviate from normal behavior. The distributed order time fractional momentum equations and fractional energy equation are derived by using the distributed order derivative and Caputo fractional derivative, respectively. The numerical simulation method for the built coupled models is carried out. The Crank-Nicolson finite difference schemes are proposed to calculate the numerical solutions of the models. A numerical example is constructed to compare the performances between numerical and exact solutions. Then, the effectiveness and feasibility of the numerical method are verified, and the effects of relevant parameters on fluid velocities and temperature are discussed, graphically. Results verify that the Hall parameters have a great influence on the fluid velocity under the action of strong magnetic field.

Conflict of interest *On behalf of all authors, the corresponding author states that there is no conflict of interest.*

Author contributions ***Yanli Qiao****: Data curation, Formal analysis, Investigation; Methodology, Software, Writing – original draft, Writing – review & editing.* ***Huanying Xu****: Methodology, Resources, Writing – review & editing, Supervision.* ***Haitao Qi****: Conceptualization, Resources, Writing –*

review & editing, Supervision, Project administration, Funding acquisition.

Acknowledgements *This work was supported by the National Natural Science Foundation of China (Grant Nos. 12172197, 12171284, and 12120101001), and the Natural Science Foundation of Shandong Province (Grant No. ZR2021ZD03).*

1 V. Tigoiu, The flow of a viscoelastic fluid between two parallel plates with heat transfer, Int. J. Eng. Sci. **29**, 1545 (1991).
2 R. Sivaraj, and B. Rushi Kumar, Unsteady MHD dusty viscoelastic fluid Couette flow in an irregular channel with varying mass diffusion, Int. J. Heat Mass Transfer **55**, 3076 (2012).
3 J. C. Yang, F. C. Li, Y. R. He, Y. M. Huang, and B. C. Jiang, Experimental study on the characteristics of heat transfer and flow resistance in turbulent pipe flows of viscoelastic-fluid-based Cu nanofluid, Int. J. Heat Mass Transfer **62**, 303 (2013).
4 J. Zhao, L. Zheng, X. Chen, X. Zhang, and F. Liu, Unsteady Marangoni convection heat transfer of fractional Maxwell fluid with Cattaneo heat flux, Appl. Math. Model. **44**, 497 (2017).
5 S. An, K. Tian, Z. Ding, and Y. Jian, Electroosmotic and pressure-driven slip flow of fractional viscoelastic fluids in microchannels, Appl. Math. Comput. **425**, 127073 (2022).
6 H. I. Andersson, MHD flow of a viscoelastic fluid past a stretching surface, Acta Mech. **95**, 227 (1992).
7 A. Raptis, C. Perdikis, and H. S. Takhar, Effect of thermal radiation on MHD flow, Appl. Math. Comput. **153**, 645 (2004).
8 M. M. Rashidi, S. Abelman, and N. Freidooni Mehr, Entropy generation in steady MHD flow due to a rotating porous disk in a nanofluid, Int. J. Heat Mass Transfer **62**, 515 (2013).
9 A. De Rosis, R. Liu, and A. Revell, One-stage simplified lattice Boltzmann method for two- and three-dimensional magnetohydrodynamic flows, Phys. Fluids **33**, 085114 (2021).
10 T. Hayat, S. B. Khan, and M. Khan, The influence of Hall current on the rotating oscillating flows of an Oldroyd-B fluid in a porous medium, Nonlinear Dyn. **47**, 353 (2007).
11 M. VeeraKrishna, G. Subba Reddy, and A. J. Chamkha, Hall effects on unsteady MHD oscillatory free convective flow of second grade fluid through porous medium between two vertical plates, Phys. Fluids **30**, 023106 (2018).
12 H. U. Rasheed, S. Islam, S. Zeeshan, W. Khan, J. Khan, and T. Abbas, Numerical modeling of unsteady MHD flow of Casson fluid in a vertical surface with chemical reaction and Hall current, Adv. Mech. Eng. **14**, (2022).
13 Y. Yin, and K. Q. Zhu, Oscillating flow of a viscoelastic fluid in a pipe with the fractional Maxwell model, Appl. Math. Comput. **173**, 231 (2006).
14 J. Zhao, L. Zheng, X. Zhang, and F. Liu, Unsteady natural convection boundary layer heat transfer of fractional Maxwell viscoelastic fluid over a vertical plate, Int. J. Heat Mass Transfer **97**, 760 (2016).
15 X. Chen, W. Yang, X. Zhang, and F. Liu, Unsteady boundary layer flow of viscoelastic MHD fluid with a double fractional Maxwell model, Appl. Math. Lett. **95**, 143 (2019).
16 R. Moosavi, R. Moltafet, and Y. Shekari, Analysis of viscoelastic non-Newtonian fluid over a vertical forward-facing step using the Maxwell fractional model, Appl. Math. Comput. **401**, 126119 (2021).
17 H. Hanif, Cattaneo-Friedrich and Crank-Nicolson analysis of upper-convected Maxwell fluid along a vertical plate, Chaos Solitons Fractals **153**, 111463 (2021).
18 A. R. Askarian, M. R. Permoon, M. Zahedi, and M. Shakouri, Stability analysis of viscoelastic pipes conveying fluid with different boundary conditions described by fractional Zener model, Appl. Math. Model. **103**, 750 (2022).
19 Y. Meng, and B. Li, On viscoelastic fluid in a vertical porous media channel with Soret and Dufour effects, Appl. Math. Lett. **124**, 107656 (2022).
20 M. A. El Kot, and Y. Abd Elmaboud, Unsteady pulsatile fractional Maxwell viscoelastic blood flow with Cattaneo heat flux through a vertical stenosed artery with body acceleration, J. Therm. Anal. Calorim. **147**, 4355 (2022).
21 C. F. Lorenzo, and T. T. Hartley, Variable order and distributed order fractional operators, Nonlinear Dyn. **29**, 57 (2002).
22 M. Caputo, and M. Fabrizio, The kernel of the distributed order fractional derivatives with an application to complex materials, Fractal Fract. **1**, 13 (2017).
23 G. Calcagni, Towards multifractional calculus, Front. Phys. **6**, 58 (2018), arXiv: 1801.00396.
24 T. M. Atanackovic, On a distributed derivative model of a viscoelastic body, Comptes Rendus Mécanique **331**, 687 (2003).
25 J. S. Duan, and X. Qiu, Stokes' second problem of viscoelastic fluids with constitutive equation of distributed-order derivative, Appl. Math. Comput. **331**, 130 (2018).
26 W. Yang, X. Chen, X. Zhang, L. Zheng, and F. Liu, Flow and heat transfer of viscoelastic fluid with a novel space distributed-order constitution relationship, Comput. Math. Appl. **94**, 94 (2021).
27 S. Yang, L. Liu, Z. Long, and L. Feng, Unsteady natural convection boundary layer flow and heat transfer past a vertical flat plate with novel constitution models, Appl. Math. Lett. **120**, 107335 (2021).
28 C. Feng, X. Si, L. Cao, and B. Zhu, The slip flow of generalized Maxwell fluids with time-distributed characteristics in a rotating microchannel, Appl. Math. Lett. **120**, 107260 (2021).
29 C. Feng, B. Li, X. Si, W. Wang, and J. Zhu, The electro-osmotic flow and heat transfer of generalized Maxwell fluids with distributed-order time-fractional characteristics in microtubules under an alternating field, Phys. Fluids **33**, 113105 (2021).
30 H. Chen, S. Lü, and W. Chen, Finite difference/spectral approximations for the distributed order time fractional reaction-diffusion equation on an unbounded domain, J. Comput. Phys. **315**, 84 (2016).
31 C. Zhu, B. Zhang, H. Fu, and J. Liu, Efficient second-order ADI difference schemes for three-dimensional Riesz space-fractional diffusion equations, Comput. Math. Appl. **98**, 24 (2021).
32 C. Wu, Numerical solution for Stokes' first problem for a heated generalized second grade fluid with fractional derivative, Appl. Numer. Math. **59**, 2571 (2009).
33 X. Yang, H. Qi, and X. Jiang, Numerical analysis for electroosmotic flow of fractional Maxwell fluids, Appl. Math. Lett. **78**, 1 (2018).
34 J. Zhao, Finite volume method for mixed convection boundary layer flow of viscoelastic fluid with spatial fractional derivatives over a flat plate, Comp. Appl. Math. **40**, 10 (2021).
35 Y. Meng, B. Li, and X. Si, Numerical analysis of fractional viscoelastic fluid problem solved by finite difference scheme, Comput. Math. Appl. **113**, 225 (2022).
36 Y. Qiao, X. Wang, H. Xu, and H. Qi, Numerical analysis for viscoelastic fluid flow with distributed/variable order time fractional Maxwell constitutive models, Appl. Math. Mech.-Engl. Ed. **42**, 1771 (2021).
37 X. Wang, Y. Qiao, H. Qi, and H. Xu, Numerical study of pulsatile non-Newtonian blood flow and heat transfer in small vessels under a magnetic field, Int. Commun. Heat Mass Transfer **133**, 105930 (2022).
38 M. VeeraKrishna, G. Subba Reddy, and A. J. Chamkha, Hall effects on unsteady MHD oscillatory free convective flow of second grade fluid through porous medium between two vertical plates, Phys. Fluids **30**, 023106 (2018).
39 X. Jiang, H. Zhang, and S. Wang, Unsteady magnetohydrodynamic flow of generalized second grade fluid through porous medium with Hall effects on heat and mass transfer, Phys. Fluids **32**, 113105 (2020).
40 D.Y. Tzou, Macro-to Microscale Heat Transfer: The Lagging Behavior, 2nd ed. (Wiley, Chichester, 2015).
41 Y. Bai, L. Huo, Y. Zhang, and Y. Jiang, Flow, heat and mass transfer of three-dimensional fractional Maxwell fluid over a bidirectional stretching plate with fractional Fourier's law and fractional Fick's law, Comput. Math. Appl. **78**, 2831 (2019).
42 M. A. Imran, F. Miraj, I. Khan, and I. Tlili, MHD fractional Jeffrey's fluid flow in the presence of thermo diffusion, thermal radiation effects with first order chemical reaction and uniform heat flux, Results Phys.

10, 10 (2018).
43 Y. Jiang, H. G. Sun, Y. Bai, and Y. Zhang, MHD flow, radiation heat and mass transfer of fractional Burgers' fluid in porous medium with chemical reaction, Comput. Math. Appl. **115**, 68 (2022).
44 T. Sandev, and Z. Tomovski, Fractional Equations and Models: Theory and Applications (Springer, Switzerland, 2019).
45 X. Hu, F. Liu, I. Turner, and V. Anh, An implicit numerical method of a new time distributed-order and two-sided space-fractional advection-dispersion equation, Numer. Algor. **72**, 393 (2016).
46 L. Liu, L. Feng, Q. Xu, L. Zheng, and F. Liu, Flow and heat transfer of generalized Maxwell fluid over a moving plate with distributed order time fractional constitutive models, Int. Commun. Heat Mass Transfer **116**, 104679 (2020).
47 J. Chen, F. Liu, V. Anh, S. Shen, Q. Liu, and C. Liao, The analytical solution and numerical solution of the fractional diffusion-wave equation with damping, Appl. Math. Comput. **219**, 1737 (2012).
48 G. Gao, Z. Sun, and H. Zhang, A new fractional numerical differentiation formula to approximate the Caputo fractional derivative and its applications, J. Comput. Phys. **259**, 33 (2014).
49 W. Ding, S. Patnaik, S. Sidhardh, and F. Semperlotti, Applications of distributed-order fractional operators: A review, Entropy **23**, 110 (2021).
50 X. Chi, H. Zhang, and X. Jiang, The fast method and convergence analysis of the fractional magnetohydrodynamic coupled flow and heat transfer model for the generalized second-grade fluid, Sci. China Math. **66**, 1 (2023).
51 Y. Liu, F. Liu, and X. Jiang, Numerical calculation and fast method for the magnetohydrodynamic flow and heat transfer of fractional Jeffrey fluid on a two-dimensional irregular convex domain, Comput. Math. Appl. **151**, 473 (2023).

具有霍尔效应的广义Maxwell流体通过无穷平板的旋转MHD流动和传热

乔艳丽, 续焕英, 齐海涛

摘要 黏弹性流体的流动和传热特性研究一直是一个备受关注的问题. 然而, 一些黏弹性流体的行为会偏离由整数阶控制方程描述的经典的流动和传热现象. 因此, 建立一种新的本构关系来研究复杂黏弹性流体是有必要的. 本文研究了霍尔效应作用下具有分布阶特性的广义Maxwell流体在无穷平板上的旋转磁流体流动和传热现象. 考虑到广义Maxwell流体流动和传热的多尺度特性和非局部性, 引入分数阶微积分理论准确地描述流动和传热机理, 导出了由时间分布阶动量方程和时间分数阶能量方程组成的分数阶控制方程. 为了计算速度和温度控制方程的数值解, 我们基于L1近似公式提出了Crank-Nicolson有限差分格式, 然后, 验证了数值方法的有效性和可行性, 并以图形形式讨论了相关参数对流体速度和温度的影响, 给出了一些结论.